Journal of Tribology and Surface Engineering ISSN: 1949-4866
Volume 3, Number 1/2

DETERMINATION OF PAD THICKNESS IN A LARGE THRUST BEARING

D. V. Srikanth*
Auroras' Engineering College,
Bhongir, Hyderabad, A. P. India

Supervisor:
Dr. K.K. Chaturvedi
Retired Sr. DGM, BHEL (R&D)
Adhoiwala, Dehradun-248001, India
ckaushal49@gmail.com

Co- Supervisor:
Dr. A. Chenna Kesava Reddy
Professor of Mechanical Engineering
JNTUH, Kukatpally
Hyderabad- 500085, India
dr_acreddy@yahoo.com

ABSTRACT

The bearing oil pressure and temperature distributions pertaining to a unique set of operating conditions are obtained by solution of the simultaneous Reynolds' and energy equations. The Vogel-Cameron equation providing for viscosity variation, hot oil carryover and numerical integration of nodal pressure were considered in the determination of the optimal pad thickness in a hydrogenerator thrust bearing. A modern finite element model using ANSYS simulates the pad deformation. A set of five pads subjected to identical loading in the thickness range of 20-60mm are considered in the analysis to determine the optimal thickness. It is observed that the compiled results of film temperature, pad deformation and Von-mises stress were satisfactory and do not vary linearly with a constant slope. The analysis for optimal pad thickness based on the above operating characteristics verifies the application of the software package. The unique interpolation of a single pad's thickness to determine the characteristics of all the bearing pads is highlighted. Unlike in previous studies this analysis is helpful in recommending the operating range and dynamics of bearing pads in hydro generators.

Keywords: temperature, deformation, Von-Mises, stress, distribution

* E-mail: dvsrikanth1@hotmail.com

NOMENCLATURE

a : oil film shape parameter
h : oil film thickness , m
h_{min} : minimum oil film thickness, m
h_o : oil film thickness at the trailing edge, m
k : composite node number
m : number of nodes on the grid in radial direction
n : number of nodes on the grid in circumferential direction
p : pressure in the oil film , Pa
q_r : flow in the radial direction per unit length, m^2/s shear force, N
q_θ : flow in the circumferential direction per unit length, m^2/s shear force, N
r_o : outer radius of the thrust pad, m
t: transit time ,B/U, s
B: circumferential length of the thrust segment,
D_i: inner diameter of the thrust bearing, m
D_o: outer diameter of the thrust bearing, m
$\dot{E}$: heat dissipation rate in the oil film, per unit area, W/m^2
G_p :gap between the pads, m
H: non-dimensional thickness of the oil film, h/h_o
L: radial length of the thrust pad, m
N: angular speed of the runner, rpm
P: non-dimensional pressure
R: radius of the runner, m
R_{cp}: radial coordinate of the centre of pressure, m
T : non-dimensional oil film temperature.
W: load on bearing, N
Z: number of pads
β : angular extent of the thrust pad.
μ: viscosity of oil , Pa.s
$\bar{\mu}$: non-dimensional viscosity
θ: angle from the leading edge, rad
θ_{cp}: angular location of the centre of pressure, rad
ρ: density of oil, kg/m^3
ω: angular speed of the runner, rad/s
$[K]$: structural stiffness matrix
$\{U\}$: nodal displacement vector
$\{R\}$: applied temperature loading vector
$\{r\}$: applied pressure loading vector

INTRODUCTION

The thrust segment enables change of the oil film geometry and maintains its optimum shape even with varied load. The principle of a thrust pad bearing is based on the convergent wedge which is formed between two relative moving surfaces. Oil is dragged into the gap due to the shearing force of the runner and squeezed out of the trailing and side edges. Combined with the advancement of digital computers recent investigations have enabled a more thorough analysis. A realistic model, of a large tilting pad is needed to develop design strategies. It is almost certain that designs will be compromised by inaccuracies in the numerical model used to develop them. To design thrust bearings, compatible with the given operating conditions, first the performance characteristics are determined. These are bearing load capacity, film thickness, stiffness, damping coefficients and film temperature as in (Chu, 2007). Numerical investigations on the tilting pad thickness for thrust bearings are very scarce to date. The objective of this study is to develop fast computational routines and to determine the pad deformation, Von-Mises stress and temperature distributions for the sample pads using ANSYS and thereby evaluate the pad thickness. Also a novel method to find the thickness of all the bearing pads based on the values of only one sector pad is formulated. Table 1 tabulates the geometry, operating conditions, material and oil properties of the test bearing for which the pad thickness is being evaluated. A good rotor model is developed if the key problems of measurement and predictability are solved. In order to do so it is essential to understand the bearing forces and rotor displacement. A comparison of the thermo-structural and plane structural analysis is done to validate the results. The aim of the pad design is to ensure its equilibrium under variation of film thickness and corresponding restoring forces.

(Vohr, 1981) made the first attempt to perform a rotor bearing analysis and include the comparison with experiments. The experimental part of his work was confined to a limited range of temperature measurements. Measurements from a laboratory apparatus and a bearing in service were presented.

There is a necessity to obtain experimental data and check the numerical predictions over a wide range of operating conditions (Yuan, 2001). A method for the calculation of temperature in the lubricant film of a thrust bearing was presented by (Ettles, 1970). This technique allowed for a simplified calculation of hot oil carry over. An analysis to propagate thermo elastic effects in time following a change in the operating load and speed was developed.

Design of tilting pad thrust bearings on the basis of isothermal solution of Reynolds' Equation was carried out by (Chaturvedi, 1984). Results of the isothermal solutions were represented by multi-nomial expressions. Performance indicators, load supported, power loss and temperature rise were calculated. Non-dimensional performance parameters and density functions for violation of constraints on film temperature and average pressure were used in the criteria function. The Nelder – Mead sequential simplex algorithm based on the optimization technique was used.

Correct bearing performance analysis depends on the accurate prediction of the oil film temperature at the inlet of a thrust pad. (Heshmat, 1986) made an important contribution in this direction. The concepts of flow and heat balances were utilized for predicting the temperature of the oil at the inlet. Experiments showed that 70-90 percent of the heat generated in a thrust pad entered the next pad and the hot lubricant adhered to the runner in the cavitation zone. Procedure and formulae for calculating the inlet temperature of thrust bearings was described.

(Gero, 1987) presented a finite element method that incorporated the temperature dependent viscosity to solve the three dimensional fluid film and pad energy equations. The systems of equations for the temperature field were solved by the iterative method. The advantage was that the parabolic or elliptic forms of the energy equation were used with the backward differencing and up winding schemes respectively. The film and pad were treated as a single continuum and their temperatures were solved simultaneously.

(Kim, 1991) carried out an analytical study incorporating simultaneous changes in the viscosity and the non-ambient inlet pressure. The quantities solved for were pressure and temperature, maximum pad temperature, load capacity, friction force, centre of pressure co-ordinates and pivot location. A significant build-up in the fore-region was found when compared with the case where pressure was assumed to be ambient.

(Zheming, 1993) developed a numerical solution for the compressible Reynolds' equation. It was an implicit scheme based on the Patankar-Spalding method used for solving heat transfer and fluid flow problems. The difficulties faced by various discretization approaches in solving slider geometries with discontinuous clearances could be overcome.

A numerical solution to the thermo-elastic hydrodynamic lubrication of a tilting pad thrust bearing was obtained by (Yang, 1997). It was based on the three-dimensional flow of a lubricant. For elastic deformation, the pad was idealized as a uniform plate with a free boundary. A conventional finite difference method displacement established the co-efficient matrix. The pressure distribution was obtained by solving the generalized Reynolds', film thickness, inlet pressure, force and momentum balance equations of the pad simultaneously. The finite difference method was carried out with the help of a sweeping scheme to obtain the temperature distribution.

(Wang Li, 2001) studied the thermo elastic hydrodynamic (TEHD) lubrication performance of the thrust bearings with Babbitt layer and/or teflon layer of large hydrogenerators was investigated by means of finite element analysis. The physical model established takes into account the lubricating oil film, thrust bearing, runner and thrust head. The thermo elastic deformation (TED) of the thrust bearing and runner was analyzed based on ADINA(T) program. It has been found that the calculated results of the thrust bearings conform well to the measured ones.

For a large thrust bearing, (Sinha, 2001) provided a realistic simulation of the Reynolds' equation. The film thickness was unknown and the centre of pressure was known together with the energy and the bending equations. The resultant film shape of the thrust pad was determined by the thermo-elastic analysis performed here.

An experimental and theoretical investigation into the effect of oil thermal properties of a tilting pad thrust bearing was conducted by (Glavatskih, 2002). Poly-a-olefin oil, ester and mineral oil were chosen for the study. They were so chosen because they had the same viscosity grade (ISO VG46) but different heat capacity, viscosity-temperature variation and thermal conductivity values. Experimental results were obtained from tests conducted on an equalizing tilting pad thrust bearing. A three dimensional theoretical TEHD model was used to analyze the oil performance. The active pad displacements due to the temperature and pressure fields were determined.

The hydrodynamic behavior of thrust bearings was analyzed by considering different dimensionless system pressure, speed and geometry by (Kurban, 2003). The load due to elastic deformation was taken into account as the bearing-load characteristics were included. The general behavior of the thrust bearing was analyzed using a proposed neural network predictor. The result gave superior performance in analyzing the behavior of a thrust bearing undergoing elastic deformation.

A finite-element method model to analyze the performance of hydrodynamic tilting-pad thrust bearing assemblies was applied by (Markin, 2003). A three dimensional model of the bearing assembly was used to assess the influence of operating conditions such as temperature across the pads. The numerical results were compared with the experimental data carried out on a spherically pivoted-pad. Good correlation was found between the model and experimental results for maximum oil film temperature, pressure and thickness. The effects of different oil types on a spring-supported thrust bearing were analyzed.

The equations of film thickness, pressure and temperature in tilting pad thrust bearings were derived in (Li, 2004). Algebraic expressions were set up for force and moment applied on the pads. The transient thermo-hydrodynamic lubrication performances of the bearings were studied. The decrease of film thickness caused by enhancing load made the film temperature rise gradually. While the load was enhanced gradually the leaning angle of the pad became greater.

(Hemmi, 2005) used computational fluid dynamics software and computed the temperature distribution in the pad by solving the heat transfer in the pad, oil and interfaces simultaneously. The thermal and stress deformation were then calculated by the FEM code and used in the oil film analysis to determine the characteristics of the bearing. Comparison of the results with the experimental ones validated the computational process.

(Jun-ling, 2005) studied the range of a bi-directional thrust bearing parameters of a large pumped-storage hydro-unit, The test of performance parameters of bi-directional thrust bearing were done at 3000T thrust bearing test stand. To get detailed information about the distribution of the oil film thickness, pressure and temperature of the test bearing pads, the characteristic of bi-directional thrust bearing were tested by means of computer data acquisition system. Valuable measurement data were obtained. The results show that bi-directional thrust bearing parameters designed are reasonable, and reliable to various bi-directional thrust bearing application.

The performance of a hydrodynamic thrust bearing with eight fixed pads was analyzed by (Dadouche, 2006). A comparison between numerical results and experimental data obtained by a thermo-hydrodynamic model was presented. An analysis of the oil temperature, applied load and rotational speed on the thrust bearing performance characteristics was carried out. Factors such as temperature field, minimum film thickness, leakage flow, and power loss were discussed. There was satisfactory agreement between the experimental and numerical results.

A theoretical analysis on the behavior of a thrust bearing was presented by (Yildrim, 2006). An adaptive finite difference method was developed to solve the Reynolds' equation for lubrication. A single one-dimensional grid was used by the model in the theoretical analysis. The altering of total lubrication load resulting from under-cutting in the thrust bearing was determined along with the oil film thickness and pressure. The bearing analysis was carried out considering different dimensionless pressure, speed and geometry. The effect of the elastic load was taken into account in the load-bearing characteristics. The general behavior of the thrust bearing was analyzed using a neural network predictor. Hydrodynamic principles were used in the design of tilting pad bearings utilized in mechanisms carrying shaft thrust or radial loads. Optimized pivot positions in the radial and circumferential directions of tilting pad thrust and radial bearings were derived by (Ni, 2007). Minimum film thickness for a given running condition of velocity, viscosity, temperature, bearing geometry and loading forces was calculated. The minimum film thickness from pressure distribution in the load-carrying analysis was solved using a simplified Reynolds' equation derived in one-dimension and applied in two dimensions.

(Ping-an, 2008) presented a method for calculating the heat conduction and thermo-elastic-deformation (TED) of the runner and thrust block by means of ANSYS program. 1/Z(Z is pad number) of runner is chosen as the model for ANSYS according to design of runner and thrust block and cycle symmetrical property, the three-dimensional contact element and the three-dimensional equivalent heat conduction element is located in space between runner and thrust block. The surface of runner is distorted due to pressure loading, the high point of deformation is on pad, and the low point of deformation is in space between pads. The radial deformation of runner is radial tilt, and the high point of deformation is in outer diameter. The surface of runner is distorted due to differential thermal deflection, the circumferential deformation is not distorted due to circumferential constant temperature, and the radial deformation of runner is convex. The whole deformation of surface of runner is radial convex, and the high point of deformation is in outer diameter, the circumferential deformation is wave.

(Jiang, 2011) studied the effects of pad elastic deformation, rotational speed, axial load, and oil viscosity grade on a tilting pad thrust bearing performance using the TEHD lubrication model. The Reynolds', viscosity–temperature, density–temperature, film thickness, energy, heat conduction and elastic deformation equations were solved simultaneously using the finite-difference method. The results showed that the maximum pressure and the minimum film thickness were reduced when pad deformation is taken into account. The heavier load increases the maximum pressure and decrease the film thickness. The temperature is slightly affected by the load.

(Zhong-de, 2011) studied the thermo-elastic-hydrodynamic lubrication performance of three gorges thrust bearing (right) with pins and double layer system have been analyzed by the finite element methods. The lubrication calculation is programmed with the finite element methods. Together with ANSYS a complete software of the thermo-elastic-hydrodynamic (TEHD) lubrication performance analysis is obtained in this paper, where the physical model includes lubricating oil film, thrust bearing, runner and thrust head. The thermo-elastic-deformation of thrust bearing and runner is analyzed with ANSYS. The calculated results are compared with the measured ones in real operation.It shows that calculated characteristics are coincident with the experimental measurement.Three Gorges thrust bearing (right) have been optimized.

Shape of the Oil Film

The film shape for a flat pad is defined by the following equation [1] for a plane, where the oil film is convergent in positive directions of x and y axes

$$h = A1 - A2x - A3y \tag{1}$$

for $x = r\sin\left(\theta - \theta cp\right)$ and $y = r\cos\left(\theta - \theta_{cp}\right) \; - r_{cp}$

i.e. the centre –of-pressure is assumed to be the origin.

Here, the coefficients A_1, A_2 and A_3 are determined by mentioning the following boundary conditions. The origin of *x* and *y* axes are located at the center–of–pressure with *y*-axis along the radius.

- It is seen in Figure 1 that film thickness at Q is the minimum film thickness h_o and using this boundary condition h_o in the equation [1].
- By using film thickness along RS and expressing γ' as the film thickness ratio in the y-direction
- Another boundary condition for use in the equation [1] is by considering the slope between points O and Q.
- Splitting γ' into two parts, one that yields uniform film thickness at the trailing edge γ_o and the other variable γ .
- Making film thickness to be invariant along the trailing edge.

The final form of the equation governing the shape of the oil film is given by

$$h = h_o\left[1 + \left(ar_{cp} \,/\, B\right)\tan\left(\beta - \theta_{cp}\right)\right] - h_o\,(ar/B)\sin\left(\theta - \theta_{cp}\right)$$

$$+ h_o\left[(a/B)\tan\left(\beta - \theta_{cp}\right) - \gamma / L\right]\left[r\cos\left(\theta - \theta_{cp}\right) - r_{cp}\right] \tag{2}$$

Equation for non-dimensional thickness of the oil film is obtained by dividing both sides with h_o and is:

$$H = h/h_o = 1 + \left(ar_{cp} \,/\, B\right)\tan\left(\beta - \theta_{cp}\right) - (a\,r/B)\sin\left(\theta - \theta_{cp}\right)$$

$$+ \left[(a/B)\tan\left(\beta - \theta_{cp}\right) - \gamma / L\right]\left[r\cos\left(\theta - \theta_{cp}\right) - r_{cp}\right] \tag{3}$$

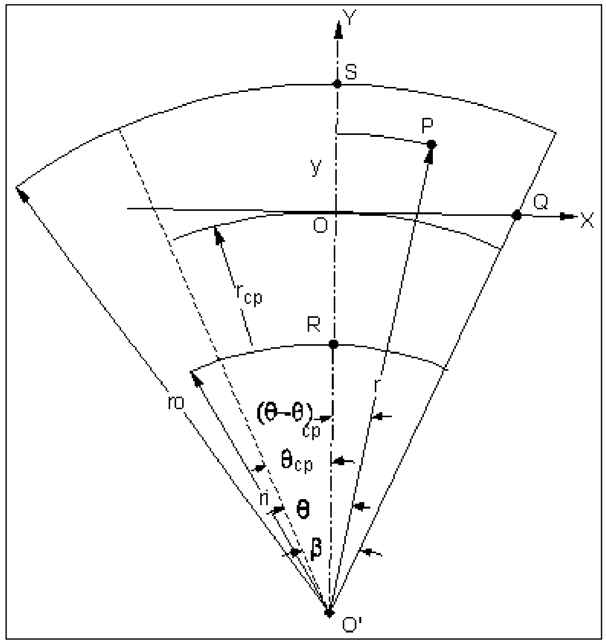

Figure 1. Shape of the oil film for a flat thrust pad.

Reynolds' Equation

The Reynolds' equation is obtained by introducing the lowest order terms of the Navier Stokes equation in the continuity equation which is then integrated across the film. The analysis of hydrodynamic thrust bearings is based on Reynolds' equation for the pressure distribution. With the increasing capacity of computers, numerical models including the influences of viscosity variations along and across the lubricating film are developed.

The Reynolds' equation for a sector-shaped thrust segment for incompressible lubricant, under steady state condition is given in equation [4]

$$\frac{\partial}{\partial r}\left[\frac{rh^3}{\mu}\frac{\partial p}{\partial r}\right]+\frac{1}{r}\frac{\partial}{\partial \theta}\left[\frac{h^3}{\mu}\frac{\partial p}{\partial \theta}\right]=6\omega r\frac{\partial h}{\partial \theta}+12r\frac{\partial h}{\partial t} \qquad [4]$$

The following assumptions are made in the analysis done herein.

1. Steady-state conditions exist in the oil film.
2. The lubricant is incompressible.
3. The lubricant is Newtonian.
4. Flow in the convergent wedge is laminar.
5. Pressure and shear effects on the viscosity are negligible.
6. Variation of the specific heat and density with pressure is negligible.

7. Wherever the oil film becomes divergent due to crowning or thermo-elastic distortion, cavitation is taken into account, by making pressure equal to zero, wherever its value is negative.

Equation [4] is non-dimensionalised by making the following substitutions

$$r = r_o\, R;\ \theta = \beta\theta \quad \mu = \mu_o\, \bar{\mu}$$
$$h = h_o H;\ \ p = \left(r_o^2\ \omega\mu_o / \beta h_o^2\right)P$$

[5]

With above substitutions, the Reynolds equation reduces to the non-dimensional form given in equation [6]:

$$2\frac{\partial}{\partial R}\left[\frac{RH^3}{\bar{\mu}}\right]\frac{\partial p}{\partial R} + \frac{2RH^3}{\bar{\mu}}\frac{\partial^2 P}{\partial R^2} + \frac{2}{\beta^2 R}\frac{\partial P}{\partial \bar{\theta}}\frac{\partial}{\partial \theta}\left[\frac{H^3}{\bar{\mu}}\right] + \frac{2}{\beta^2 R}\frac{H^3}{\bar{\mu}}\frac{\partial^2 P}{\partial \bar{\theta}^2} = 12R\frac{\partial H}{\partial \theta} + 24\, R\ \beta\,\frac{\partial H}{\partial t} \qquad [6]$$

Equation [7] with better numerical accuracy is obtained when the first derivatives in the above equation are converted into second derivative terms.

$$\frac{\partial^2}{\partial R^2}\left[\frac{RH^3 p}{\bar{\mu}}\right] + \frac{RH^3}{\bar{\mu}}\frac{\partial^2 P}{\partial R^2} + \frac{1}{R\beta^2}\frac{H^3}{\bar{\mu}}\frac{\partial^2 P}{\partial \bar{\theta}^2} - \frac{P}{R\beta^2}\frac{\partial^2}{\partial \bar{\theta}^2}\left[\frac{H^3}{\bar{\mu}}\right]$$
$$- P\frac{\partial^2}{\partial R^2}\left[\frac{RH^3}{\bar{\mu}}\right] + \frac{1}{R\beta^2}\frac{\partial^2}{\partial \bar{\theta}^2}\left[\frac{H^3 P}{\bar{\mu}}\right] = 12R\frac{\partial H}{\partial \theta} + 24R\beta V \qquad [7]$$

Energy Equation

Thermal effects caused due to viscous shearing of lubricant layers can limit performance in a number of ways. The heat generated lowers the film viscosity resulting in decreased load capacity. The flow of oil transports this heat to other parts of the film. This heat generation and transport is governed by the energy equation. The pressures and temperatures are formulated in terms of partial differences. Equation [8] gives the energy equation for laminar flow and incompressible lubricant.

$$C_p\rho\ \left[q_r\,\frac{\partial T}{\partial r} + q_\theta\,\frac{1}{r}\frac{\partial T}{\partial \theta}\right] = \dot{E} \qquad [8]$$

where equations [9], [10] and [11] give radial, circumferential flow and heat dissipation rate.

$$q_r = -\frac{h^3}{12\ \mu}\frac{\partial p}{\partial r} \qquad [9]$$

$$q_\theta = \frac{r\omega h}{2} - \frac{h^3}{12\mu}\frac{1}{r}\frac{\partial p}{\partial \theta} \qquad [10]$$

$$\dot{E} = \frac{\mu}{h}(\omega r)^2 + \frac{h^3}{12\mu}\left[\left(\frac{1}{r}\frac{\partial p}{\partial \theta}\right)^2 + \left(\frac{\partial p}{\partial r}\right)^2\right] \quad [11]$$

The Vogelpohl – Cameron equation [12] gives the variation of viscosity with temperature and is used in the iteration.

$$\mu = \mu_0 e^{A/(T+95)} \quad [12]$$

It is included in the iteration process. The circumferential sides are assumed to be insulated and thus an adiabatic situation exists. The boundary conditions for temperatures for these two sides are given in equation [13]:

$$\begin{aligned} T_{m+1,j} &= T_{m-1,j} \\ T_{i-1,j} &= T_{i+1,j} \end{aligned} \quad [13]$$

The energy equation containing the terms $\frac{\partial T}{\partial r}$ and $\frac{\partial T}{\partial \theta}$ is set up in finite differences to express $\frac{\partial T}{\partial r}$ in terms of $\frac{\partial T}{\partial \theta}$ and the local heat dissipation. The first order of the equation indicates that it is an initial value or propagation problem. The temperature along the whole leading edge is specified so that initial values of $\frac{\partial T}{\partial r}$ are also known. The following equations express $\frac{\partial T}{\partial r}$ with variation of temperature between adjacent nodes in the circumferential and radial directions.

$$\frac{\partial T}{\partial r} = \frac{1}{2dr}\left[4T_{k+1} - 3T_k - T_{k+2}\right] \text{ in the forward difference form} \quad [14]$$

$$\frac{\partial T}{\partial r} = \frac{1}{2dr}\left[T_{k+1} - T_{k-1}\right] \text{ in the central difference form} \quad [15]$$

$$\frac{\partial T}{\partial r} = \frac{1}{2dr}\left[T_{k-2} + 3T_k - 4T_{k-2}\right] \text{ in the backward difference form} \quad [16]$$

$\frac{\partial P}{\partial \theta}$ and $\frac{\partial P}{\partial R}$ are expressed in a similar way as $\frac{\partial T}{\partial r}$ with the variation of pressure.

Thus the temperature of the downstream node is determined as

$$\frac{\partial T}{r\partial \theta} = \frac{\left[\frac{\dot{E}}{\rho Cp} - \frac{h^3}{12\mu}\frac{\partial p}{\partial r}\frac{\partial T}{\partial r} \right]}{\left[\frac{r\omega h}{2} - \frac{h^3}{12\mu}\frac{1}{r}\frac{\partial p}{\partial \theta} \right]} \quad [17]$$

where, $\frac{\partial T}{r\partial \theta} = \frac{1}{2r_k \Delta \theta}\left[T_{k+1} - T_{k-1}\right]$ [18]

The lubricant entering the wedge at the inlet edge is heated to some extent by the hot runner in the inter-pad space. This lubricant also consists of some oil pre-heated in the preceding pad and some oil from the bath to make up for the oil lost due to side leakage. Thus, the actual inlet temperature in the oil film is higher temperature to the bulk oil temperature. This effect has been investigated in detail by (Ettles, 1970) experimentally and analysed. The hot oil carry over effect is represented as

$$T_{out} = T_{sup} + \Delta T\left(\frac{2-k}{2-2k}\right) \quad [19]$$

where $k = \frac{T_{in} - T_{supp}}{T_{run} - T_{supp}}$ [20]

assumed in our study to be = 0.83

$$T_{in} = T_{out} - \Delta T \quad [21]$$

COUPLED THERMAL-STRUCTURAL DEFORMATION EQUATION

The thermal structural deformation equation is given by equation [22]

$$[K]\{U\} = \{R\} + \{r\} \quad [22]$$

where $[K]$ is structural stiffness matrix, $\{U\}$ is nodal displacement vector, {R} is applied temperature loading vector and {r} is applied pressure loading vector.

The hexahedral solid 226 element is used to mesh the pad thermo-structural deformation model. It has up to twenty nodes with up to five degrees of freedom per node. The structural capabilities are only elastic including large deflection and stress stiffening.

Figure 2 shows its geometry, node locations, and coordinate system. The units are specified through the EMUNIT command. The KEYOPT (1) function value determines the nodal loading on these elements. In the plane analysis nodal forces are input per unit of depth for a plane analysis. For the axi-symmetric analysis it is on a full 360° basis. The KEYOPT (1) function determines the element DOF set and corresponding force. It is set equal to the sum of the field keys. In the structural-thermal analysis for example to indicate the sum of the structural and thermal field keys KEYOPT (1) is set as 1+10= 11.

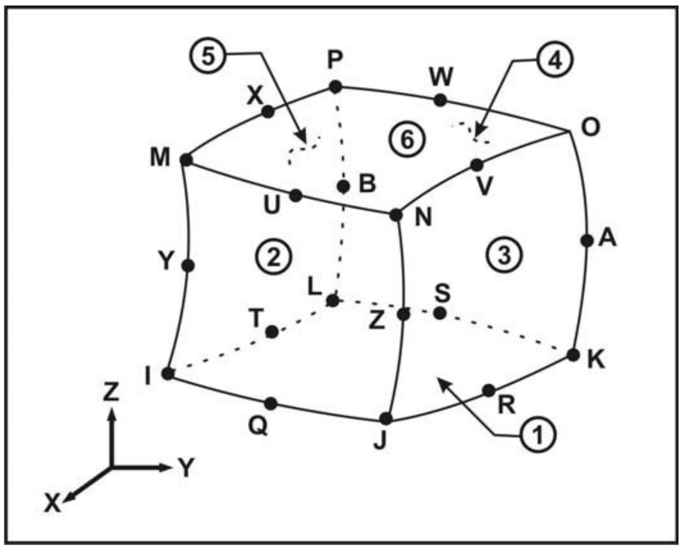

Figure 2. Solid 226 element geometry.

Computational Methodology

In this research, the TEHD model employs the finite difference model to solve the 2D modified Reynolds'and energy equations and obtains the thermal-elastic deformations of the pad with the finite element software ANSYS11.0. In the oil film domain the governing Reynolds' equation for hydrodynamic lubrication is solved for a laminar flow regime. A finite difference discretization of the thrust pad is done by considering a total of 81 nodes in the form of a 9 × 9 grid. The truncated Taylor series expansion for three successive grid points is used to approximate the derivatives in the Reynolds's equation. The central difference form is used to determine functional values of adjacent nodes on either side in order to evaluate the required derivatives. The above equations are written for every node and a resultant set of simultaneous linear algebraic equations are obtained. These are solved by matrix inversion and multiplication. The energy equation which governs the generation of heat and transport is also solved simultaneously using the same finite difference method and pad discretization. As the energy equation depends upon the pressure gradient, it is solved simultaneously with the Reynolds' equation using the same grid. The initial values of uniform temperature and viscosity distribution are used to solve Reynolds' equation. q_r and q_θ are then determined from equations [9] and [10]. Equation [8] is then solved for $T(r,\theta)$ and hence μ (T). Reynolds' equation is then resolved for pressure using the new distribution for viscosity. This iterative scheme converged quickly. Thus once the temperature of the bulk oil in the housing is known and temperature rise has been calculated, the inlet temperature, the outlet temperature and the runner temperature can be calculated. In this procedure, taking hot oil carry over effect into consideration the successive values of temperature downstream in the flow direction are obtained in a single sweep.

In the 3D pad model and pre-processing phase the cross-sectional geometry, material properties and load data listed in Table 1 are input for the authors' data. A similar structural analysis is conducted for Yuan's data. The first step in the analysis is the solid model development and meshing.

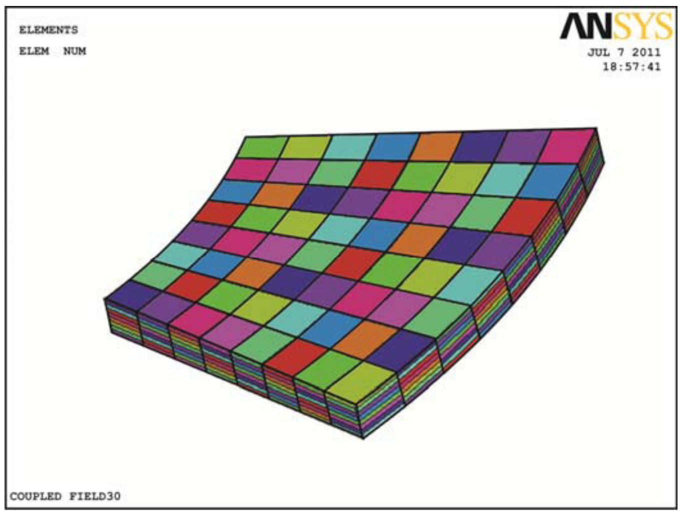

Figure 3. Elemental plot of the pad.

Table 1. Thrust Bearing Geometry

	Yuans' data	Authors' data	Zhong De's data
Outer Diameter (m)	1.168	1.275	5.200
Inner Diameter(m)	0.711	0.75	3.500
Number of Pads	12	6	24
Thickness (mm)	41.1	40	64+115+240
Groove width(mm)	52.3	84	-
Type of support	Spring	Spring	Double layer pin type
Operating Conditions			
Load (MN)	2.124	3	47.56
Rotational speed (rads/s)	52.4	14.28	17.08
Oil pot temperature (º C)	70	40	38.6
Oil Properties			
ISO grade	46	68	68

γ (cSt) at 40 º C	48	73	73
γ (cSt) at 100 º C	6.70	10.7	10.7
ρ (g/m) at 15 º C	0.873	0.861	0.861
Pad mechanical Properties			
Young's modulus (GPa)	195		
Poisson's ratio	0.29		
Density (Kg/m^{3})	7850		
Pad thermal Properties			
Thermal expansion/ °C		$12.2e^{-6}$	
Thermal conductivity (W/m-K at 10°C)		42.6	
Specific heat (J/kg-K)		473	
Heat transfer coefficient for inner surface		$6.015e^{-4}$	
Heat transfer coefficient for outer surface		$30e^{-6}$	

The axi-coordinate system is used to create the model in ANSYS. It is done using key points and joining consecutive lines, creating areas and operating about the axis. The model is next meshed using the hexahedral Solid 226 elements and simulated for a load step. For the coupled thermo-structural deformation the elemental plot of the pad is shown in Figure 3.

There exist 8 elements in radial, 8 in circumferential and 8 along the thickness to a total of 512 hexahedral Solid 226 elements in the deformation function. An identical mesh on the sliding face was used in the FEM model in order to facilitate the data transfer between the THD model and the FEM model.

The axi-symmetric boundary condition is used in applying the pressure and load to the bottom surface area A2. The convection heat transfer from the areas A1, A3, A4 and A6 of Figure 4 is considered. The bulk oil temperature and convection film coefficient value are 40°C and $4e^{6}$ respectively.

The heat flux values obtained from the energy equation and those of the elemental nodes at the bottom surface of the pad are identical. Radiation heat transfer from the pad is neglected.

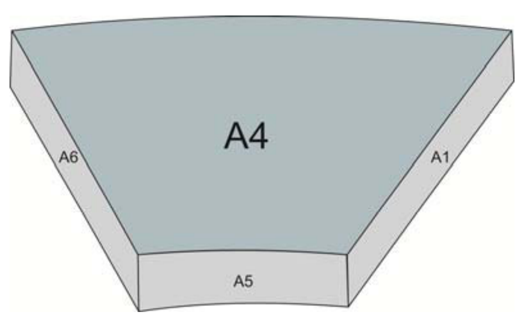

Figure 4. Areas for applicable loads and heat transfers.

Results of the deformation function are viewed by applying a load step. To view the results, functions of plot result, counter plot, nodal solution and the displacement vector are applied. The calculated thermal and elastic deformation were used to modify the oil film profile and then obtain new pressure and temperature distributions which were transferred next into the FEM model again.

RESULTS AND DISCUSSIONS

Figure 5 shows how the 40mm thick pad deforms to a maximum at the bottom and outer circumferential edge in the coupled field analysis. It is obvious that the thermal deformations in the bearing pad forms a convex shape as a result of the temperature gradient through its thickness. At the same time, under the compensation of springs the elastic deformations in the bearing pad forms a concave shape as a result of hydrodynamic pressure, thus minimizing the total pad deflection as well as maximizing bearing capacity.

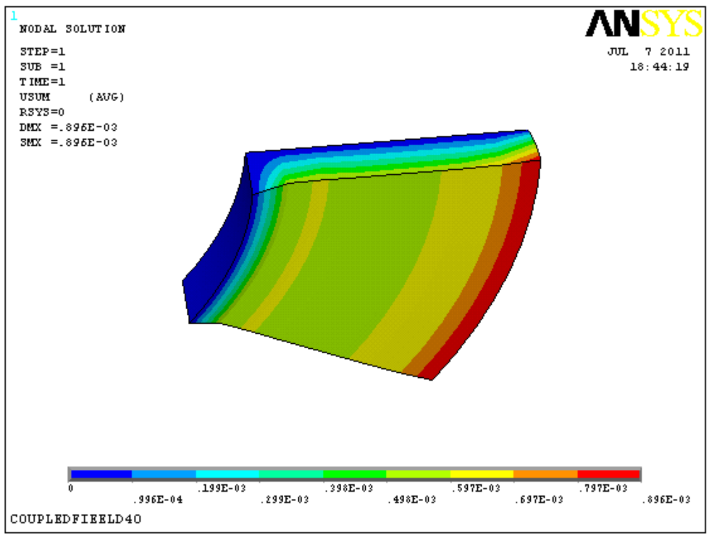

Figure 5. Coupled field deformation distribution.

The values of coupled field deformations for the author's pad and that obtained from (Zhong De, 2011) as listed in Table 1 are 0.896E-3 and 0.466E-3. In Figure 6 the plane structural deformation of the 40mm pad for Yuans' dimensions is 0.107e^{-}4 and that of Zhong De's pad is 0.186 e-4. These are in agreement inspite of the variation in size, operating conditions and type of supports. In a word this is because the deformations on the pad are of the same order of magnitude with oil film thickness which in both cases is in the order of 6μm and tends to form a satisfactory oil film profile.

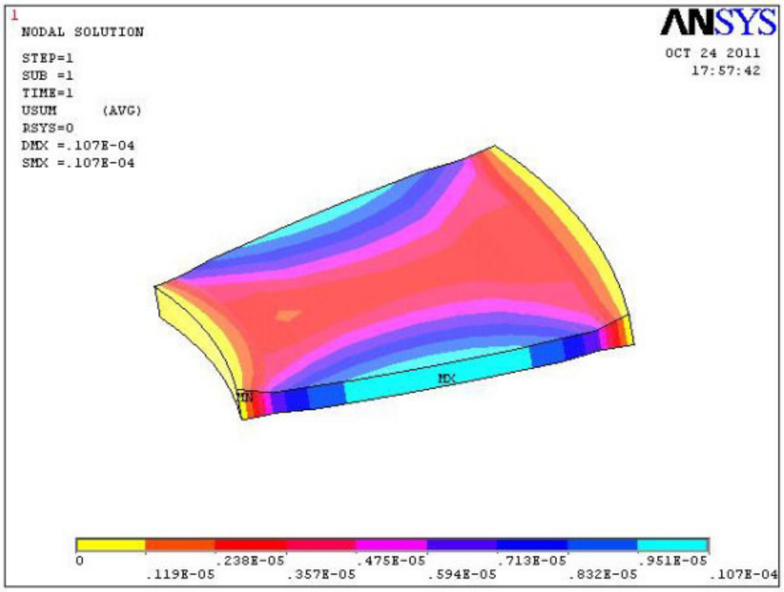

Figure 6. Structural deformation distribution.

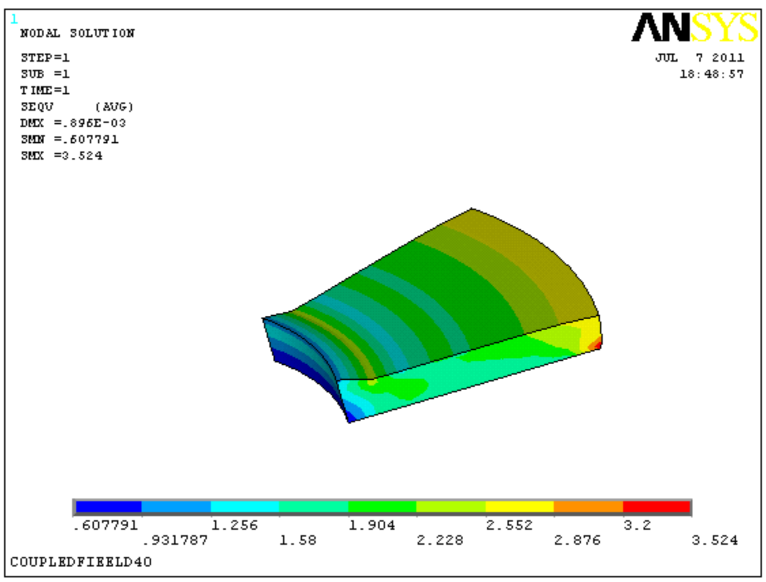

Figure 7. Von-Mises stress distribution.

The Von-Mises stress distribution for the 40mm pad is shown in Figure 7. It varies from a minimum of 0.61 N/mm^2 to a maximum of 3.524 N/mm^2.

A thorough thickness analysis based on the numerical operating characteristics of a set of pads' is attempted and conducted. Pads of 20mm, 30mm, 40mm, 50mm and 60mm thickness and same material are subjected to identical thermal and structural loading conditions. The corresponding deformation, temperature and Von-Mises stress functions using ANSYS are plotted separately for the authors' coupled and Yuans' structural fields respectively.

Figures 8, 9 and 10 clearly show the variation of deformation, temperature and Von-Mises stress for increasing pad thickness. These functions do not increase linearly with constant slope as the pad thickness increases from 20mm to 60mm. In the 30 mm-40 mm thickness range the slope of the deformation and temperature line are maximum for the thermo-structural analysis. This indicates that the 40mm thick pad has the best ability to withstand high deformation and temperature when compared to thicknesses in the preceding 20mm-30mm and successive 40mm-60mm ranges. In addition the maximum deformation and Von-Mises stress values for the 40mm pad are $0.896e^{-3}$ mm and 35 N/mm^2 which are respectively greater than and equal to the mean maximum deformation and stress values of all the pads. In the plane structural analysis the deformation and Von-Mises stress functions show a decrease with increase in thickness and have mean values at 40mm.

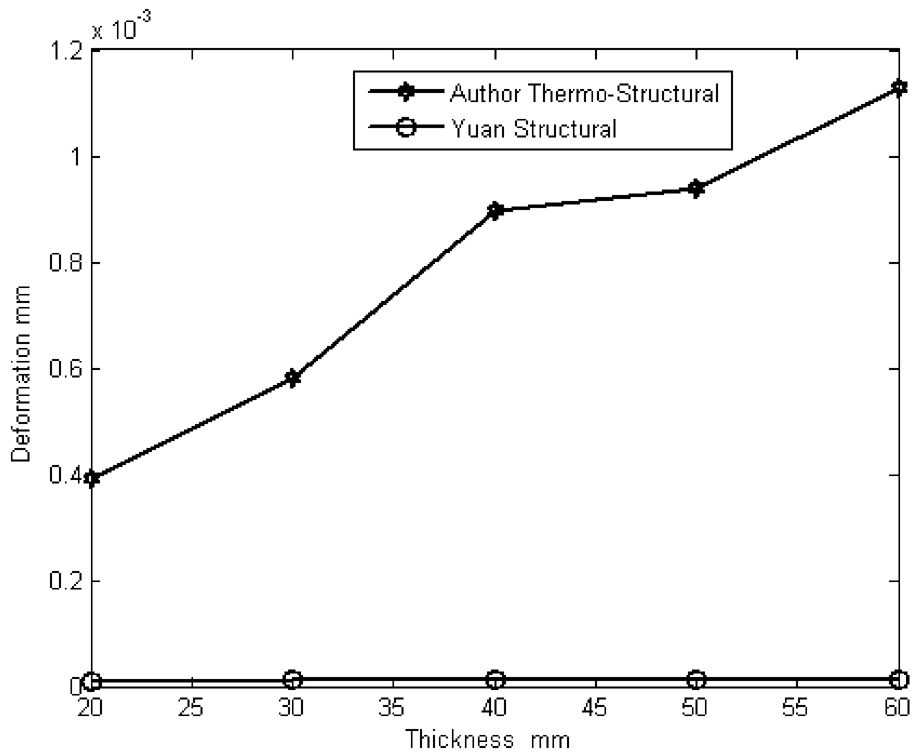

Figure 8. Deformation vs thickness.

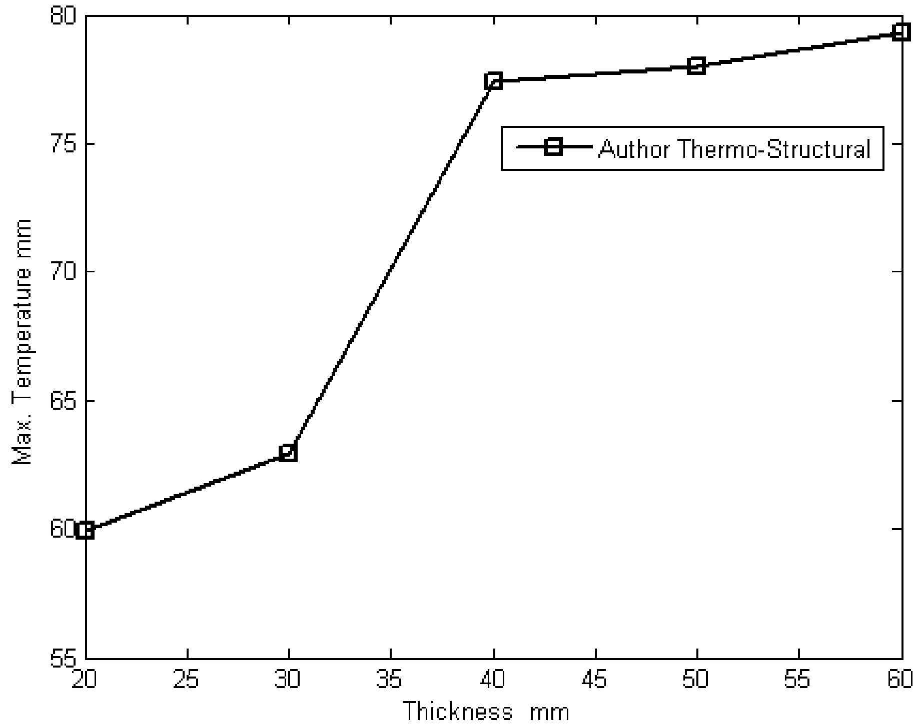

Figure 9. Temperature vs thickness.

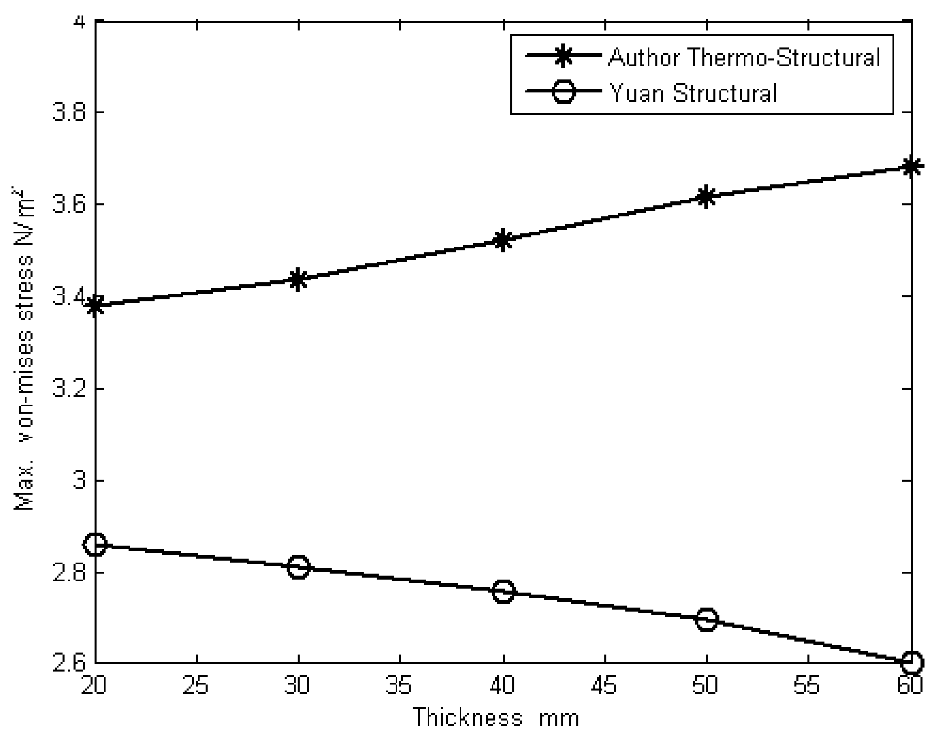

Figure 10. Von-Mises stress vs thickness.

The above study validates the recommendation of the 40mm thick pad as best suitable for the given working conditions. It also shows the importance and accuracy of thermal stresses in pad selection. A database for the thickness characteristics of all the pads can be developed with this analysis.

CONCLUSION

The modified Reynolds' and Energy equations in two dimensions were formulated for determining the oil pressure and temperature distributions. Load computation by numerical integration of nodal pressure and corresponding viscosity cum temperature variations in bearing oil were considered in the determination of the optimal pad thickness of a large thrust bearing. A modern three dimensional FEM model using ANSYS simulates the plane structural and coupled thermo-structural deformation of the pad. The compiled results of oil film temperature, pad deformation and Von-mises stress distribution were found satisfactory in terms of computer time and convergence criteria. As a validation the structural and coupled deformation values pertaining to the author's, Yuan's and Zhong De's bearing geometry and conditions were found in agreement.

The significance of interpolating the thickness characteristics of all the pads by simulating the load and thickness of one pad is discussed. An in depth study reveals that the 40 mm thickness gives best bearing performance and is recommended for use in the bearing pressure range of 3 to 6 MPa.

The relationship between pad thickness and pad performance is not linear. In between a thin pad and a thick one, there exists an optimum pad which gives excellent performance. The basic difference when compared to earlier studies is in the use of a unique ANSYS analysis to determine the optimal pad thickness.

REFERENCES

Chaturvedi. K..K.. (1984), "Computer Program for Optimization of Tilting Pad Thrust Bearing Design for CAD Application", *National Conference on Industrial Tribology*, Hyderabad, 141 – 148.

Chu, H. M. (2007), "Shape Optimum Design of Slider Bearings using Inverse Methods", *Tribology International,* 40, 906-914.

Dadouche, A., Fillon, M. and Dmochowski, W. (2006), "Performance of a Hydrodynamic fixed Geometry Thrust Bearing- Comparison between Experimental Data and Numerical results", *Tribology Transactions*, 49(3), 419-426.

Ettles, C. (1970), "Hot Oil Carry Over in Thrust Bearings", *Proceedings of I Mech. Eng..,* 184(3L), 75-81.

Ettles. C. M. M. (1982), "Transient Thermo elastic effects in Fluid Film Bearings", *Wear,* 79, 53-71.

Gero L. R., and Ettles C.M.M. (1987), "A three Dimensional Thermo-hydrodynamic Finite Element Scheme for Fluid Film Bearings ", *STLE Tribology Transactions,* 31(2), 182-191.

Glavatskih, S.B., Fillon, M. and Larsson, R. (2002), "The Significance of Oil Thermal Properties on the Performance of a Tilting – Pad Thrust Bearing" *ASME, Journal of Triboogy.,* 124(2), 377 – 386.

Hemmi, M., Hagiya, K., Ichisawa, K. and Fujita S. (2005), "Computation of Thermal Deformation of Thrust Bearing Pad Concerning the Convection by Non- Uniform Oil Flow", World Tribology Congress III, Washington D.C, 61-62.

Heshmat, H. and Pinkus, O. (1986), "Mixing Inlet Temperatures in Hydrodynamic Bearings", *Journal of Tribology*, 108(2), 231-241.

Jiang, X., Wang, J., Fang, J. (2011), "Thermal Elastohydrodynamic Lubrication Analysis of Tilting Pad Thrust Bearings, Proceedings. I-MechE, Part J: *Journal of Engineering Tribology*, 225(2), 51-57.

Jun-ling,W., Zhong-de, W., Yu-tian, S., Su, C., (2005), "Test Study of Bi-directional Thrust Bearing" , *Large Electric Machine and Hydraulic Turbine,*1.

Kim K. W. and Rodkiewicz, C.M. (1991), "On the Thermal Effects in the Design of Tilting – Pad Bearings Subjected to Inlet Pressure Build-Up", *ASME , Journal of Tribology,* 113(3), 526-532.

Kurban, A.O. and Yildrim, S. (2003), "Analysis of a Hydrodynamic Thrust Bearing with Elastic Deformation using a Recurrent Neural Network", *Tribology International,* 36(12), 943-948.

Li, Z and Qing, D. (2004), "Study on Transient Lubrication Performance of Thrust Bearings with Tilting Pads Set on Variation Load", Zhongguo Jixie Gongcheng/ China *Mechanical Engineering*, 15(15), 1326-1328.

Markin, D., McCarthy, D.M.C. and Glavatskih, S.B. (2003), "A FEM Approach to Simulation of Tilting-Pad Thrust Bearing Assemblies", *Tribology International,* 36(11), 807-814.

Ni, W., Griffiths, C., Bartholme, D. and Hergert, R. (2007), "Two Dimensional Analytical Analysis of Fluid Film Thickness on Pivoted Tilting Pad Bearings", Powertran and Fluid systems , *Conference and Exhibition*, Chicago , IL , USA .

Ping-an, L. and Zhong-de, W. (2008), "Analysis of Thermo-elastic Deformation of Runner and Thrust Block for Hydro-generators", *Large Electric Machine and Hydraulic Turbine*, 2(4).

Sahin, Y. (2006) "Design of an Artificial Neural Network Predictor for Analysis of a Hydrodynamic Thrust Bearing System", *Industrial Lubricationn and Tribology*, 58(2), 89-94.

Sinha, A.N., Athre, K. and Biswas, S. (2001), "Non-linear Solution of Reynolds Equation for Thermoelastohydrodynamic Analysis of a Thrust Pad Bearing", *Industrial Lubrication and Tribology*, 53, 202-210.

Vohr, J.H. (1981), "Prediction of the Operating Temperature of Thrust Bearings", *ASME Journal of Lubrication Technology*, 103, 97-106.

Wang Li, Q. , Zhong De, W. , , Da Zhuang , Q., Yu lin, Q., (2001), "Analysis of Thermoelastic Hydrodynamic Lubrication Performance of Thrust Bearings for Large Hydrogenerators", *Tribology*, 2(16).

Yang, P. and Rodkiewicz, C.M. (1997), "On the Numerical Analysis to the Thermoelastohydrodynamic lubrication of a Tilting Pad Inclusive of Side Leakage", *Tribology Transactions*, 40(2)259-266.

Yuan, J.H., Medley, T.B. and Ferguson, J.H. (2001), “Spring supported Thrust Bearings Used in Hydro-Electric Generators: Comparison of experimental data with numerical predictions”, *Tribol. Trans.,* 44(1), 27-34.

Zheming, Z. and Wenkang, S. (1993), “A New Method for the Numerical Solution of the Reynolds’ Equation at Low Spacing” , *ASME, Journal of Tribology*, 115(1), 83-87.

Zhong-de, W. and Zhang, H. (2011), “Performance Analysis of Thrust Bearing for Three Gorges Generator”, *Large Electric Machine and Hydraulic Turbine*, 2(3).